3

Analysis of a Coupled-Mass Microrheometer

David Cheneler
University of Birmingham
United Kingdom

1. Introduction

Many large companies, especially those involved in chemical synthesis, for instance those that manufacture personal care products or pharmaceuticals, are increasingly reliant on high throughput screening techniques to develop their next generation products. This may be to facilitate product optimisation or quality control of existing processes. Many of these products are viscoelastic in nature and require sophisticated rheological techniques to determine their properties (Hansen & Quake, 2003). However, current rheological techniques are not well suited to high throughput characterisation of the generally small volumes of liquid available (Kumble, 2003). Recently a number of devices, known as microrheometers, have been fabricated with the ability to determine the properties of small samples of viscoelastic fluids (Cheneler, 2011, Crecea et al., 2009, Christopher et al., 2010). These devices are generally designed to dynamically manipulate isolated drops of fluid, usually contained in liquid bridges (Cheneler, 2011, Christopher et al., 2010), and are not in a form that is easily integrated into a commercial automated process, precluding high-throughput analysis.

One of the limitations to the development of microrheometers and their subsequent integration into commercial processes is the difficulty in modelling microfluidic systems. The issue is that only a few of the possible fluid geometries that can be realised in useful experimental set-ups lend themselves to analytical mathematical investigation. As such this causes, in the design of microrheometers, the analysis of the fluid mechanics to be highly idealised or restricted to simple cases (Christopher et al., 2010). Most microfluidic systems can be modelled in a numerical fashion, whether it is using finite element analysis, molecular dynamics or computational fluid dynamics (Sujatha et al. 2008). This would suffice if the microfluidic system was in isolation, but in a microrheometer, the system is integrated into a micro electro-mechanical system (MEMS). In such devices the mechanical dynamics, the electrical circuit analysis and fluid mechanics are all coupled together. These three facets require different techniques to model them and in general these techniques are incompatible. Therefore in order to get accurate quantitative data from a microrheometer, each aspect of the analysis has to be performed in a more consistent form. This requires there to be an analytical solution to the equations describing the microfluidics and for the solution to be in a form that can be coupled into the analysis of the rest of the system. This will allow the complete deterministic response of the microrheometer to be known.

The purpose of this chapter is to describe the complete system analysis of a new kind of coupled-mass microrheometer and show how such a device can be integrated into a real production process. It will be shown how the fluid mechanics can be fully analysed, starting from the basic governing equations, as a sinusoidal viscoelastic squeeze flow problem. The solution of which is coupled with the dynamical and electrical analysis of the microrheometer and a deterministic and quantitative method of measuring the viscoelastic fluid properties is given.

2. Principles of the coupled-mass microrheometer

The microrheometer to be described here is an oscillating coupled-mass device driven by a comb drive actuator (see Fig. 1). Its response is measured capacitively using a structure akin to the comb drive actuator. It incorporates a microfluidic channel through which the sample is delivered and removed, allowing simple integration with production lines and automated systems. At present this microrheometer has not been fabricated, but to do so would require only minor modifications to the standard techniques used to presently fabricate silicon-based comb-drive actuated oscillators as discussed by Lee (Lee, 2011).

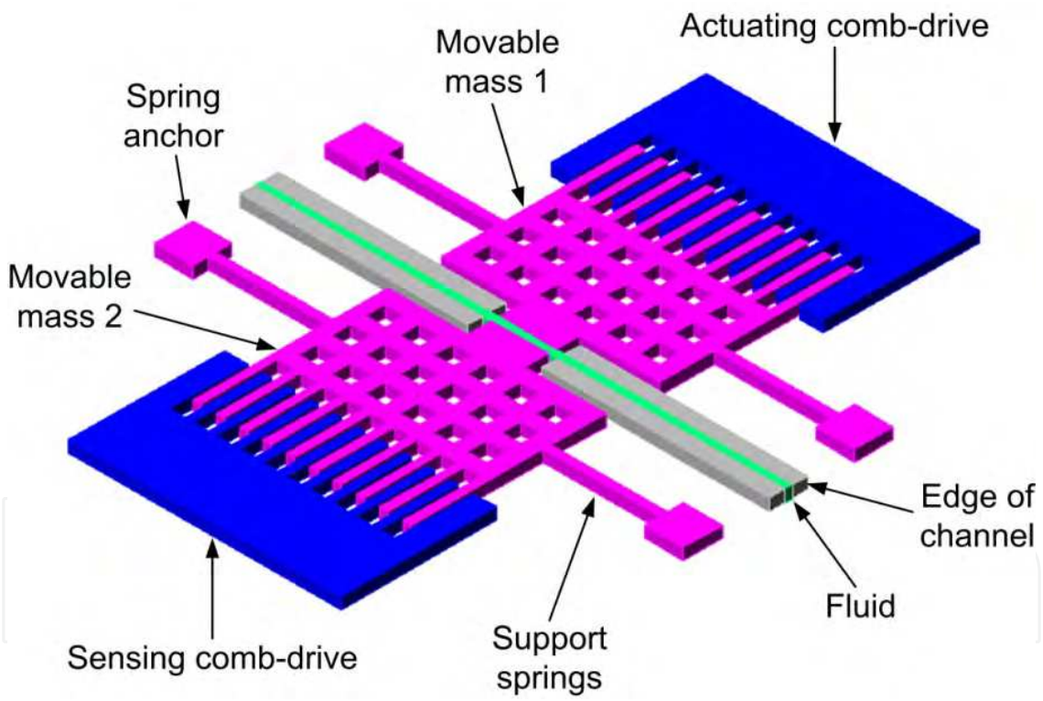

Fig. 1. A schematic of the coupled-mass microrheometer

The premise is that when a signal is applied to the actuating comb drive, it exerts a force on mass one (see Fig. 2) causing it to oscillate at a prescribed frequency. This squeezes between two parallel plates the fluid in the channel, which is formed from a compliant membrane. The fluid in turn applies a force to the second mass which then moves at the same frequency as the first. This uses the phenomena whereby micro-oscillators on the same chip suffer from unintentional cross-talk and frequency locking (Wei, 2009). Whilst normally this would be a problem, here it is beneficial. The movement of the second mass is detected by

measuring the change in capacitance of the sensing comb drive. Knowing the force applied to the first mass and the response of the second mass allows for the determination of the fluids viscoelastic properties.

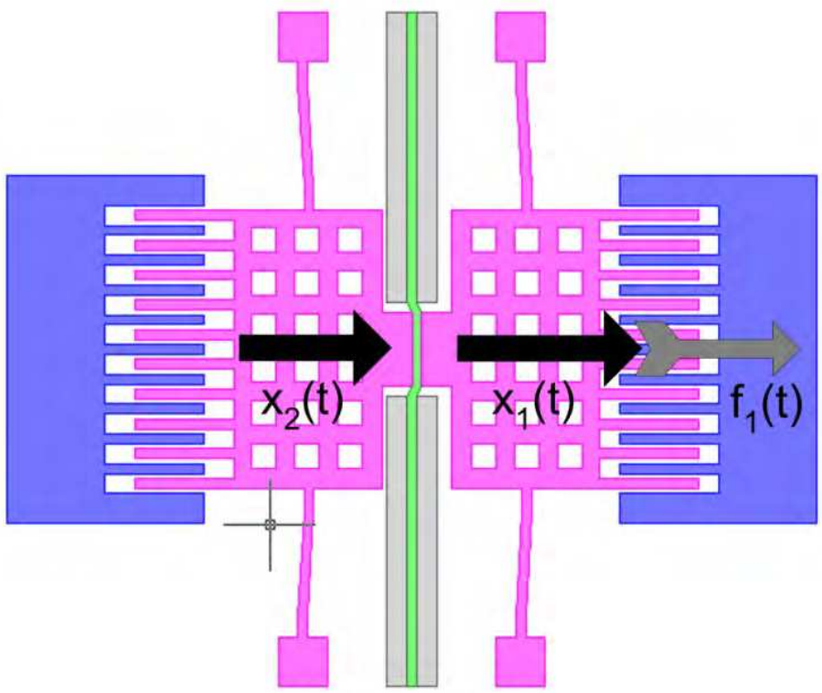

Fig. 2. A schematic showing the dynamics of the microrheometer. Here x(t) denotes the displacement of each of the masses respectively and $f_1(t)$ denotes the force applied by the actuating comb drive

3. Theoretical aspects

As stated, the microrheometer described here is an oscillating coupled-mass device (see Fig. 3) and as such lends itself to be modelled using a lumped-mass analysis (Wei, 2009). This method assumes that the dynamics of the device is identical to that of an equivalent system of masses, springs and dashpots which represent the inertial, restorative and dissipative components of the device respectively. In order for this analysis to represent the entire system however, the fluid mechanics and electrical circuitry will also have to be represented as spring, dashpots and external forces in a consistent fashion. This will be discussed in more fully in the subsequent sections.

3.1 Dynamics of a coupled-mass microrheometer

In lumped-mass analysis, it is assumed that the device can be represented by a system of masses, springs and dashpots. By this it is meant that the parameters such as stiffness and damping factors are constants so that forces are linearly dependent on velocity or displacement for instance. This is generally the case when displacements are small (Rao, 2010) and nonlinearities in the motion are negligible. In this instance, it is assumed that all the parameters are defined as constants as shown Fig. 3:

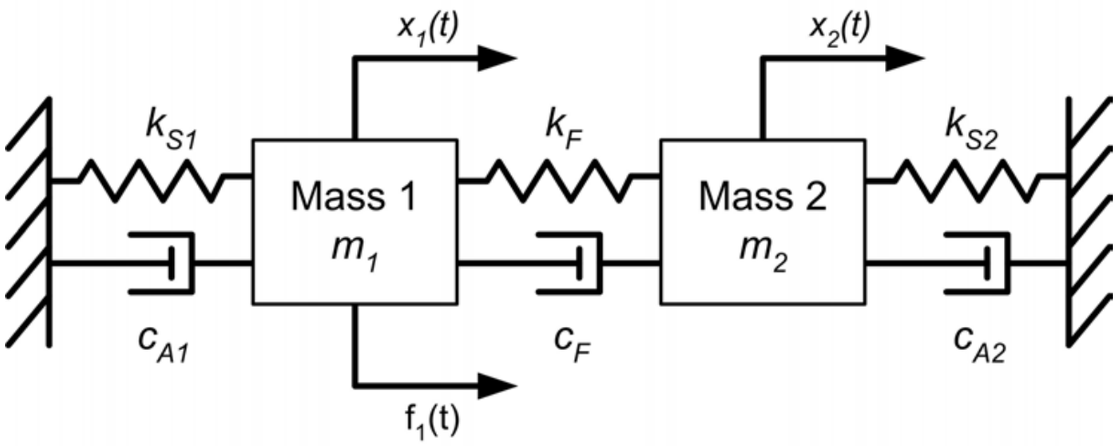

Fig. 3. A schematic of the equivalent lumped-mass system. k_S and c_A denote the stiffness of the support springs and the air damping associated with each of the masses, m. k_F and c_F denote the effective stiffness and damping parameters which are a function of the fluids viscoelastic properties

The coupled equations of motion for such a system is:

$$\begin{aligned} m_1\ddot{x}_1 + (c_{A1} + c_F)\dot{x}_1 - c_F\dot{x}_2 + (k_{S1} + k_F)x_1 - k_F x_2 &= f_1(t) \\ m_2\ddot{x}_2 - c_F\dot{x}_1 + (c_F + c_{A2})\dot{x}_2 - k_F x_1 + (k_F + k_{S2})x_2 &= 0 \end{aligned} \tag{1}$$

where one dot signifies velocity and two dots denote acceleration. These equations need to be solved to give x_2. This is the instantaneous position of mass 2 which is the value measured by the sensing electrode as shown in Fig. 1. The fluid properties can therefore be calculated from this value. As the force applied to mass 1 is sinusoidal and has the form $f_1 = Fe^{i\omega t}$ where F is the amplitude of the applied force and ω is the angular frequency, the responses of mass 1 and 2 can be assumed to have the form $x_1 = X_1 e^{i\omega t}$ and $x_2 = X_2 e^{i\omega t}$ where X_1 and X_2 are the amplitudes of the displacements of mass 1 and 2 respectively. Differentiating and substituting these factors into eq. 1 allows the equations to be represented in matrix form:

$$\begin{bmatrix} -\omega^2 m_1 + i\omega(c_{A1} + c_F) + (k_{S1} + k_F) & -i\omega c_F - k_F \\ -i\omega c_F - k_F & -\omega^2 m_2 + i\omega(c_F + c_{A2}) + (k_F + k_{S2}) \end{bmatrix} \begin{bmatrix} X_1 \\ X_2 \end{bmatrix} = \begin{bmatrix} F \\ 0 \end{bmatrix} \tag{2}$$

From eq. 2 the following factors can be defined:

$$Z_1 = -\omega^2 m_1 + k_{S1} + i\omega c_{A1} \tag{3}$$

$$Z_2 = -\omega^2 m_2 + k_{S2} + i\omega c_{A2} \tag{4}$$

$$Z_F = k_F + i\omega c_F \tag{5}$$

These are the mechanical impedances (Rao, 2010) related to mass 1, mass 2 and the fluid respectively. Note that all the coefficients are known in eqs. 3 and 4 and the coefficients in

eq. 5 are those related to the dynamic properties of the fluid and are hence the coefficients to be measured. Substituting these impedances into eq. 2 allows for the following simplification:

$$\begin{bmatrix} Z_1 + Z_F & -Z_F \\ -Z_F & Z_2 + Z_F \end{bmatrix} \begin{bmatrix} X_1 \\ X_2 \end{bmatrix} = \begin{bmatrix} F \\ 0 \end{bmatrix} \tag{6}$$

Multiplying both sides of eq. 6 by the inverse of the impedance matrix gives the amplitudes X_1 and X_2. X_2 can be shown to be:

$$X_2 = \frac{Z_F F}{(Z_1 + Z_F)(Z_2 + Z_F) - Z_F^2} \tag{7}$$

This can be simplified to:

$$X_2 = \frac{Z_F F}{Z_1 Z_2 + (Z_1 + Z_2) Z_F} \tag{8}$$

Therefore the unknown fluid impedance can be given as:

$$Z_F = k_F + i\omega c_F = \frac{X_2 Z_1 Z_2}{F - X_2(Z_1 + Z_2)} \tag{9}$$

As evidenced in eqs. 3, 4 and 7, Z_1, Z_2 and X_2 are complex. This means the displacement of mass 2 can be given as:

$$x_2 = |X_2|(\cos\phi + i\sin\phi)e^{i\omega t} \tag{10}$$

where ϕ is the phase between the displacement of mass 2 and the force (and related voltage) applied to mass 1 and $|X_2|$ is the absolute (measured) amplitude of the displacement of mass 2. $X_2 = |X_2|(\cos\phi + i\sin\phi)$ is the form that needs to be substituted into eq. 9 as all the values are measured and therefore known. The effective stiffness and damping parameters due to the fluids viscoelastic properties are given by the real and imaginary components of eq. 9, thus:

$$k_F = \mathrm{Re}\left(\frac{X_2 Z_1 Z_2}{F - X_2(Z_1 + Z_2)} \right) \tag{11}$$

$$c_F = \frac{1}{\omega}\mathrm{Im}\left(\frac{X_2 Z_1 Z_2}{F - X_2(Z_1 + Z_2)} \right) \tag{12}$$

If the air damping in eq. 1 is negligibly small, eqs. 11 and 12 become:

$$k_F = \frac{|X_2|(k_{S1} - \omega^2 m_1)(k_{S2} - \omega^2 m_2)\left[F\cos\phi - |X_2|\left[(k_{S1} + k_{S2}) - \omega^2 (m_1 + m_2) \right]\cos(2\phi) \right]}{F^2 - 2|X_2|F\left[(k_{S1} + k_{S2}) - \omega^2 (m_1 + m_2) \right] + \left(|X_2|\left[(k_{S1} + k_{S2}) - \omega^2 (m_1 + m_2) \right] \right)^2} \tag{13}$$

$$c_F = \frac{|X_2|(k_{S1}-\omega^2 m_1)(k_{S2}-\omega^2 m_2)\left[F\sin\phi - |X_2|\left[(k_{S1}+k_{S2})-\omega^2(m_1+m_2)\right]\sin(2\phi)\right]}{F^2 - 2|X_2|F\left[(k_{S1}+k_{S2})-\omega^2(m_1+m_2)\right]+\left(|X_2|\left[(k_{S1}+k_{S2})-\omega^2(m_1+m_2)\right]\right)^2} \quad (14)$$

It should be noted that eq. 10 can be expanded to give:

$$x_2 = |X_2|\left[\cos\phi\cos\omega t - \sin\phi\sin\omega t + i\left(\cos\phi\sin\omega t + \sin\phi\cos\omega t\right)\right] \quad (15)$$

This simplifies to:

$$x_2 = |X_2|\left(\cos(\omega t+\phi) + i\sin(\omega t+\phi)\right) \quad (16)$$

As the force applied to mass 1 will actually be the real component of f_1, i.e. $f_1 = \mathrm{Re}(Fe^{i\omega t}) = F\cos(\omega t)$, the actual response of mass 2 that is measured is the real component of eq. 16:

$$x_2 = |X_2|\cos(\omega t+\phi) \quad (17)$$

Therefore given that x_2 is measured, f_1 is what was applied and everything in Z_1 and Z_2 is known, k_F and c_F, and hence the fluids viscoelastic properties, can be explicitly calculated.

3.2 Derivation of the viscoelastic fluid dynamics

The squeezing of a Newtonian fluid between two plates was first detailed analytically by Reynolds (Reynolds, 1886) although it wasn't solved at that time for viscoelastic materials or for fluids being squeezed between rectangular plates. There have been many subsequent studies into viscoelastic squeeze flow due to its pertinence to lubrication (Bell et al., 2005). These studies have mostly concentrated on axisymmetric squeeze flow (Engmann et al., 2005) or constant load/velocity squeezing when considering rectangular plates and has generally been limited to plane strain cases (Denn & Marrucci, 1999). Therefore here a detailed derivation of the sinusoidal squeezing of a viscoelastic fluid between two parallel rectangular plates will be given. This will be achieved with a particular view of producing the relevant coefficients needed for the analysis in §3.1. To solve the squeeze flow problem consider the inertialess Navier-Stokes and continuity equations for Newtonian liquids in Cartesian coordinates (Reynolds, 1886):

$$\frac{dp}{dx} = \mu\left(\frac{d^2u}{dx^2}+\frac{d^2u}{dy^2}+\frac{d^2u}{dz^2}\right) \quad (18)$$

$$\frac{dp}{dy} = \mu\left(\frac{d^2v}{dx^2}+\frac{d^2v}{dy^2}+\frac{d^2v}{dz^2}\right) \quad (19)$$

$$\frac{dp}{dz} = \mu\left(\frac{d^2w}{dx^2}+\frac{d^2w}{dy^2}+\frac{d^2w}{dz^2}\right) \quad (20)$$

$$0 = \frac{du}{dx} + \frac{dv}{dy} + \frac{dw}{dz} \tag{21}$$

where z is on one of the surfaces of the channel in the direction of relative motion, y is on the same surface in the direction perpendicular to relative motion and x is mutually perpendicular (see Fig. 4). u, v and w are the velocity components in the x, y and z directions respectively. p is the pressure distribution in the channel.

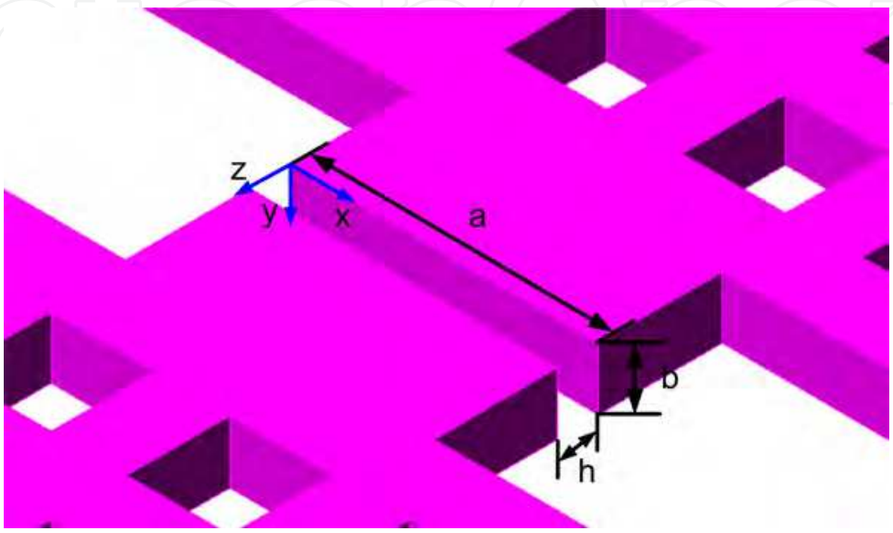

Fig. 4. A close up of the geometry between the plates squeezing the fluid. Fluid and channel have been omitted for clarity. The blue arrows denote the coordinate system used

As the channel width is small, w will be small compared to u and v, and the variations of u and v in the directions x and y are small compared with their variations in the z direction. The equations for the interior of the film then become:

$$\frac{dp}{dx} = \mu \frac{d^2u}{dz^2} \tag{22}$$

$$\frac{dp}{dy} = \mu \frac{d^2v}{dz^2} \tag{23}$$

$$\frac{dp}{dz} = 0 \tag{24}$$

These equations are subject to the following boundary conditions:

$$\begin{aligned} z = 0 &\Rightarrow u = 0, \;\; v = 0, \;\; w = 0 \\ z = h &\Rightarrow u = 0, \;\; v = 0, \;\; w = V \end{aligned} \tag{25}$$

Where h is the instantaneous width of the channel and V is the relative velocity of the sides. As eq. 24 shows the pressure to be independent of z, eqs. 22 and 23 are directly integrable. Integrating gives:

$$u = \frac{1}{2\mu}\frac{dp}{dx}(z-h)z \tag{26}$$

$$v = \frac{1}{2\mu}\frac{dp}{dy}(z-h)z \tag{27}$$

Differentiating these equations with respect to x and y respectively and substituting into the continuity equation (eq. 21) gives:

$$\frac{dw}{dz} = -\frac{1}{2\mu}\left[\frac{d}{dx}\left\{\frac{dp}{dx}(z-h)z\right\} + \frac{d}{dy}\left\{\frac{dp}{dy}(z-h)z\right\}\right] \tag{28}$$

Integrating from z = 0 to z = h and using the boundary conditions in eq. 25 gives:

$$\frac{d^2p}{dx^2} + \frac{d^2p}{dy^2} = \frac{12\mu V}{h^3} \tag{29}$$

This is the equation that needs to be solved to calculate the pressure distribution in the channel so that the force required to squeeze the fluid at a certain velocity can be found. This is possible because this is Poisson's equation of the form:

$$\nabla^2 p = -q(x,y) \tag{30}$$

Therefore we can assume it to have a solution of the form (Strauss, 2007):

$$p(x,y) = \sum_{m=1}^{\infty}\sum_{n=1}^{\infty} C_{mn}\phi_{nm}(x,y) \tag{31}$$

where $\phi_{nm}(x,y)$ are the eigenfunctions of the related Helmholtz equation:

$$\nabla^2\phi + \lambda\phi = 0 \tag{32}$$

Substituting eq. 31 into eq. 30 gives:

$$\sum_{m=1}^{\infty}\sum_{n=1}^{\infty} C_{mn}\nabla^2\phi_{nm}(x,y) = -q(x,y) \tag{33}$$

From eq. 32 we get:

$$\nabla^2\phi_{mn} = -\lambda\phi_{mn} \tag{34}$$

This can be solved using separation of variables by assuming a solution of the form:

$$\phi(x,y) = X(x)Y(y) \tag{35}$$

Substituting this into eq. 34 gives:

$$X''(x)Y(y) + X(x)Y''(y) + \lambda X(x)Y(y) = 0 \tag{36}$$

Upon rearranging, this leads to:

$$\frac{X''(x)}{X(x)} = -\frac{Y''(y)}{Y(y)} - \lambda = -\mu \tag{37}$$

This results in two ODEs and their associated boundary conditions:

$$X''(x) + \mu X(x) = 0, \quad X(0) = 0, \quad X(a) = 0 \tag{38}$$

$$Y''(y) + (\lambda - \mu) Y(y) = 0, \quad Y(0) = 0, \quad Y(b) = 0 \tag{39}$$

Where a is the width of the silicon plates and b is the depth (see Fig. 4). The boundary conditions are equivalent to stating the pressure is zero outside the gap between the plates. Eq. 38 has the solution:

$$X_m(x) = \sin\left(\frac{m\pi x}{a}\right), \quad m = 1,2,3... \tag{40}$$

So that:

$$\mu = \frac{m^2\pi^2}{a^2} \tag{41}$$

Similarly:

$$Y_n(y) = \sin\left(\frac{n\pi y}{b}\right), \quad n = 1,2,3... \tag{42}$$

And:

$$\lambda - \mu = \frac{n^2\pi^2}{b^2} \tag{43}$$

Combining eq. 41 and eq. 43 gives:

$$\lambda_{nm} = \pi^2\left(\frac{m^2}{a^2} + \frac{n^2}{b^2}\right), \quad m,n = 1,2,3... \tag{44}$$

Substituting eq. 40 and eq. 42 into eq. 35 gives:

$$\phi_{mn} = \sin\left(\frac{m\pi x}{a}\right)\sin\left(\frac{n\pi y}{b}\right), \quad m,n = 1,2,3... \tag{45}$$

Combining eqs. 33 and 34 give:

$$q(x,y) = \sum_{m=1}^{\infty}\sum_{n=1}^{\infty} C_{mn}\lambda_{mn}\phi_{mn}(x,y) \tag{46}$$

Everything in eq. 46 is known except for the coefficients C_{mn}. These can be found using the generalised Fourier series in two variables (Strauss, 2007) thus:

$$C_{mn} = \frac{12}{ab\lambda_{mn}} \int_0^b \int_0^a q(x,y) \sin\left(\frac{m\pi x}{a}\right) \sin\left(\frac{n\pi y}{b}\right) dxdy, \quad m,n = 1,2,3 \tag{47}$$

As $q(x,y) = -\frac{12\mu V}{h^3}$ (from comparing eqs. 29 and 30) this becomes:

$$C_{mn} = \frac{48\mu V}{mn\pi^2 h^3 \lambda_{mn}} \left[\cos(m\pi)\cos(n\pi) - \cos(m\pi) - \cos(n\pi) + 1\right], \quad m,n = 1,2,3 \tag{48}$$

Substituting this into eq. 31 gives:

$$\begin{aligned} p(x,y) = \sum_{m=1}^{\infty} \sum_{n=1}^{\infty} \frac{48\mu V}{mn\pi^2 h^3 \lambda_{mn}} \left[\cos(m\pi)\cos(n\pi) - \cos(m\pi) - \cos(n\pi) + 1\right] \times ... \\ ... \sin\left(\frac{m\pi x}{a}\right) \sin\left(\frac{n\pi y}{b}\right), \quad m,n = 1,2,3... \end{aligned} \tag{49}$$

The force is found by integrating this pressure over the top surface thus:

$$\begin{aligned} F_F = \sum_{m=1}^{\infty} \sum_{n=1}^{\infty} \frac{48\mu V}{mn\pi^2 h^3 \lambda_{mn}} \left[\cos(m\pi)\cos(n\pi) - \cos(m\pi) - \cos(n\pi) + 1\right] \times ... \\ ... \int_0^b \int_0^a \sin\left(\frac{m\pi x}{a}\right) \sin\left(\frac{n\pi y}{b}\right) dxdy, \quad m,n = 1,2,3... \end{aligned} \tag{50}$$

This equals:

$$F_F = \sum_{m=1}^{\infty} \sum_{n=1}^{\infty} \frac{48ab\mu V}{mn\pi^4 h^3 \lambda_{mn}} \left[\cos(m\pi)\cos(n\pi) - \cos(m\pi) - \cos(n\pi) + 1\right]^2, \quad m,n = 1,2,3 \tag{51}$$

This is the force required to squeeze a Newtonian liquid between two parallel rectangular plates at a known velocity. To see if this is a sensible result, compare it to the well-known force required to squeeze the fluid between two parallel circular plates, known as the Stefan-Reynolds equation (Bell et al. 2005):

$$F_{FC} = \frac{3\pi\mu R^4 V}{2h^3} \tag{52}$$

In eqs. 51 and 52, is can be seen that the solutions for the rectangular and for the circular plates are both linearly dependent on the viscosity and the velocity and are both inversely proportional to the cube of the gap between the plates. Furthermore, if it assumed that the dimensions of the rectangular plates make them square and that the radius of the circular plates are such that the surface area of the square and circular plates are equal, as can be seen in Fig. 5, where the two plates are far apart the solution for the circular and rectangular plates are nearly identical as is expected.

The damping coefficient for a Newtonian liquid squeezed between two rectangular plates can then given simply as:

$$c = \sum_{m=1}^{\infty}\sum_{n=1}^{\infty}\frac{48ab\mu}{mn\pi^4 h^3 \lambda_{mn}}\left[\cos(m\pi)\cos(n\pi)-\cos(m\pi)-\cos(n\pi)+1\right]^2, \quad m,n=1,2,3 \tag{53}$$

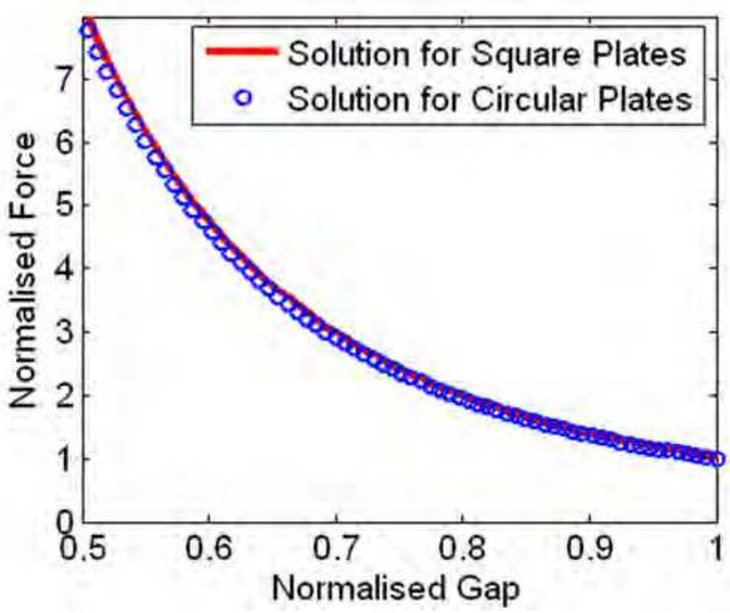

Fig. 5. Comparison between the solution for squeeze flow between rectangular plates, eq. 51, and the classical Stefan-Reynolds equation, eq. 52, for circular plates. For the purposes for comparison it is assumed the plates are square with the same surface area as the circular plates

For a viscoelastic liquid it is necessary to take into account the memory of the liquid. Therefore the force must take on the form (Bird et al., 1987):

$$F_F = \sum_{m=1}^{\infty}\sum_{n=1}^{\infty}\frac{48ab}{mn\pi^4 h^3 \lambda_{mn}}\int_{-\infty}^{t} G(t-t')\frac{dh}{dt'}dt'\left[\cos(m\pi)\cos(n\pi)-\cos(m\pi)-\cos(n\pi)+1\right]^2 \tag{54}$$
$$m,n=1,2,3...$$

If the boundaries of the channels are oscillating, the channel width has the form (Bell et al., 2005):

$$h(t) = \bar{h} + \varepsilon e^{i\omega t} \tag{55}$$

where $\bar{h}$ is the average gap, ω is the angular frequency and ε is the amplitude of oscillation. And by substituting:

$$t - t' = \xi \tag{56}$$

into the integral found in eq. 54, we obtain:

$$\int_{-\infty}^{t} G(t-t')\frac{dh(t')}{dt'}dt' = i\omega\varepsilon e^{i\omega t}\int_{0}^{\infty} G(\xi)e^{-i\omega\xi}d\xi \tag{57}$$

$G(\xi)$ represents the memory function of the material. If the fluid inside the channel is assumed to be a Maxwell liquid, this is defined as (Macosko, 1994):

$$G(t) = G_0 e^{-\frac{t}{\tau}} \tag{58}$$

where G_0 is the shear modulus and τ is the relaxation time. Substituting into eq. 57 and integrating gives:

$$i\omega\varepsilon e^{i\omega t}\int_{0}^{\infty} G_0 e^{-\frac{\xi}{\tau}} e^{-i\omega\xi}d\xi = G_0\frac{1}{1/\tau + i\omega}\frac{dh}{dt} = \left(\eta' - i\frac{G'}{\omega}\right)\frac{dh}{dt} \tag{59}$$

where η' is the dynamic viscosity and G' is the storage modulus. Substituting this result back into eq. 54 gives the force required to squeeze a viscoelastic fluid sinusoidally between two rectangular plates as:

$$F_F = \varepsilon e^{i\omega t}(iG''+G')\sum_{m=1}^{\infty}\sum_{n=1}^{\infty}\frac{48ab}{mn\pi^4\bar{h}^3\lambda_{mn}}\left[\cos(m\pi)\cos(n\pi)-\cos(m\pi)-\cos(n\pi)+1\right]^2 \tag{60}$$
$$m,n = 1,2,3...$$

G'' is the loss modulus of the fluid and is defined as $G'' = \omega\eta'$. It is the storage and loss modulus, i.e. G' and G'' that is of rheological importance (Macosko, 1994) and are therefore the most commonly measured dynamic viscoelastic properties. Separating the components of eq. 60 that are in-phase with the displacement and velocity respectively gives the final stiffness, k_F, and damping, c_F, coefficients for the liquid that are to be used in §3.1:

$$k_F = \sum_{m=1}^{\infty}\sum_{n=1}^{\infty}\frac{48abG'}{mn\pi^4\bar{h}^3\lambda_{mn}}\left[\cos(m\pi)\cos(n\pi)-\cos(m\pi)-\cos(n\pi)+1\right]^2 \tag{61}$$

$$c_F = \sum_{m=1}^{\infty}\sum_{n=1}^{\infty}\frac{48abG''}{mn\pi^4\bar{h}^3\lambda_{mn}}\left[\cos(m\pi)\cos(n\pi)-\cos(m\pi)-\cos(n\pi)+1\right]^2 \tag{62}$$

3.3 Electrical considerations

As shown in Fig. 1, the system is actuated using a capacitive lateral comb-drive. The force caused by applying a voltage to the comb-drive actuator is proportional to the change in capacitance and to the square of the applied voltage. Specifically for a comb-drive actuator this becomes (Lee, 2001):

$$F_{cd}(t) = \frac{1}{2}\frac{\partial C}{\partial x}v(t)^2 = n\frac{\varepsilon t}{g}v(t)^2 \tag{63}$$

where C is the capacitance of the comb-drive, ε is the permittivity of the medium between the teeth, t is the thickness of a tooth, g is the gap between opposing teeth and n is the number of teeth. $v(t)$ is the applied voltage. As the force is proportional to the square of the voltage, if the voltage was purely a sinusoidal signal, the force will have double the frequency of the voltage. Therefore it is common practice (Lee, 2011) to add a DC bias voltage to the applied voltage signal, i.e.:

$$v(t) = V_{DC} + V_{AC}\cos(\omega t) \tag{64}$$

where V_{DC} is the amplitude of the DC bias voltage and V_{AC} is the amplitude of the sinusoidal voltage. An example of the circuitry that could be used in this instance is shown in Fig. 6:

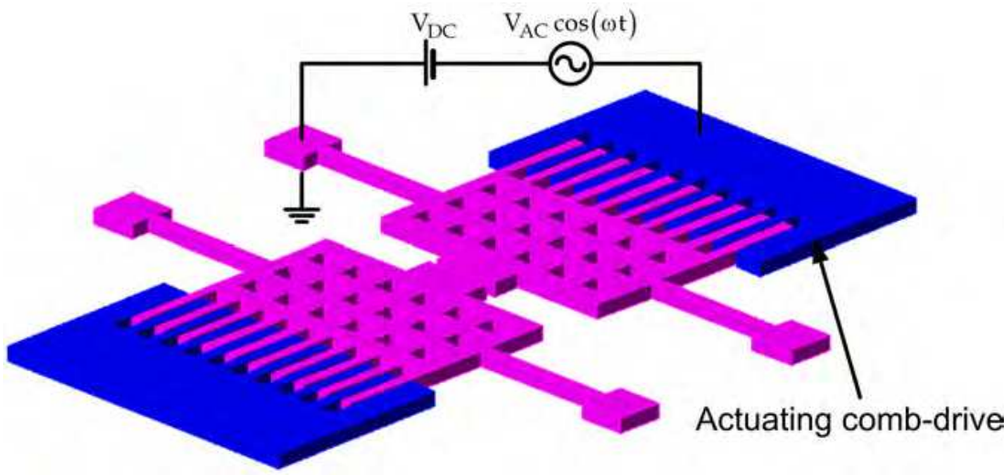

Fig. 6. A schematic of the circuitry for the actuating comb-drive. Note the moving masses are grounded through the anchors on the springs

The force therefore becomes:

$$F_{cd}(t) = n\frac{\varepsilon t}{g}\left(V_{DC} + V_{AC}\cos(\omega t)\right)^2 = n\frac{\varepsilon t}{g}\left({V_{DC}}^2 + 2V_{DC}V_{AC}\cos(\omega t) + {V_{AC}}^2\cos^2(\omega t)\right) \tag{65}$$

When $V_{DC} >> V_{AC}$ eq. 65 can be approximated as:

$$F_{cd}(t) = F_C + F\cos(\omega t) \tag{66}$$

where F_C is a constant force and F is the amplitude of the applied force as used in eqs. 11 and 12. These constants can be shown to be:

$$F_C = n\frac{\varepsilon t}{g}\left({V_{DC}}^2 + \frac{{V_{AC}}^2}{2}\right) \tag{67}$$

$$F = 2n\frac{\varepsilon t}{g}V_{DC}V_{AC} \tag{68}$$

The additional constant force naturally has an effect which wasn't considered in §3.1. Plugging a constant force into eq. 2 gives the static displacement of mass 1 and 2 as:

$$X_{1S} = \frac{k_{S2} + k_F}{k_{S1}k_{S2} + k_F(k_{S1} + k_{S2})} F_C \tag{69}$$

$$X_{2S} = \frac{k_F}{k_{S1}k_{S2} + k_F(k_{S1} + k_{S2})} F_C \tag{70}$$

However as the fluid in the channel is defined as a Maxwell liquid, and k_F is proportional to the storage modulus as shown in eq. 60, k_F becomes zero as the force is constant. This is because the storage modulus varies as (Macosko, 1994):

$$G'(\omega) = \frac{G_0\tau^2\omega^2}{\tau^2\omega^2 + 1} \tag{71}$$

where G_0 is the shear modulus introduced in eq. 57 and τ is the characteristic relaxation time of the liquid. Therefore:

$$X_{1S} = \frac{F_C}{k_{S1}} \tag{72}$$

$$X_{2S} = 0 \tag{73}$$

It is important to note is that the average gap between the plates, $\bar{h}$, is therefore smaller by a factor X_{1S}.

4. Discussion

For the sake of simplifying the discussion of the theory, it is assumed that the channel is filled with a simple Maxwell liquid whose relaxation modulus is described by the data given in Fig. 7.

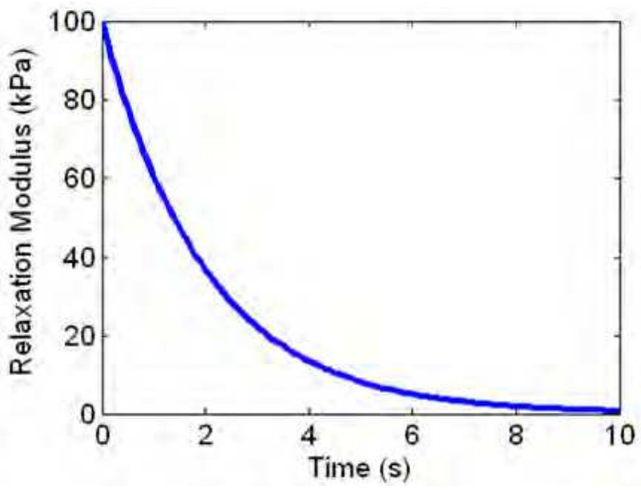

Fig. 7. Typical relaxation data for a simple Maxwell fluid

Fitting a Prony series to this data, such as that given by eq. 57, shows that the behaviour of this liquid can be described by a single relaxation time constant and a single shear modulus. For this hypothetical liquid these happen to be τ = 2 s and G_0 = 100 kPa. These constants suggest that the storage and loss moduli of the liquid should take the form of that shown in Fig. 8:

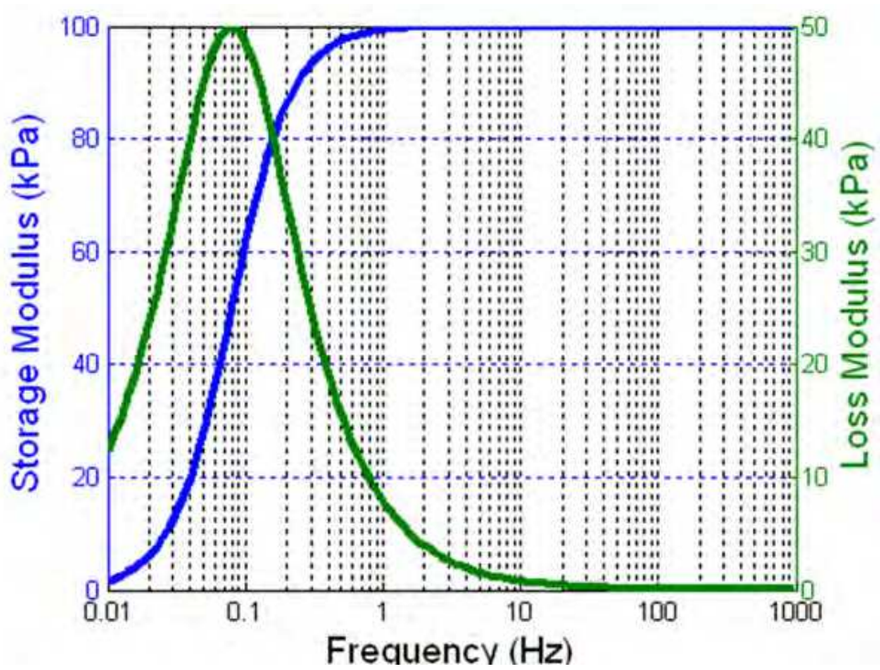

Fig. 8. The resultant dynamic properties of the simple Maxwell Fluid

Here the storage modulus is defined as in eq. 71 and the loss modulus is defined as (Macosko, 1994):

$$G''(\omega) = \frac{G_0 \tau \omega}{\tau^2 \omega^2 + 1} \tag{74}$$

The mechanical parameters of the coupled-mass microrheometer should also by known by design. Here, for simplicity it shall be assumed that $m_1 = m_2$ = 4x10^{-8} kg, $k_{S1} = k_{S2}$ = 600 N/m and $c_{A1} = c_{A2}$ = 0.1 kg/s. Also for the electrical parameters it will be assumed that n = 100, t = 50 µm and g = 0.1 µm. The applied voltages are V_{DC} = 100 V and V_{AC} = 1 V. This means the sinusoidal force given by eq. 68 is 9 µN and the constant force given by eq. 67 is 443 µN. Therefore if the original channel width was 10µm, $\bar{h}$ = 10.75 µm. As the measured material properties are calculated from eqs. 61 and 62, which are inversely proportional to the cube of the average channel width, ignoring the effects of the static deflection given by eq. 72 could lead to substantial errors. In this case the error in the measured storage and loss moduli would have been *c.a.* 24%.

Given these values, the displacement of mass 2 – the displacement that will be measured, can be predicted. The results are shown in Fig. 9.

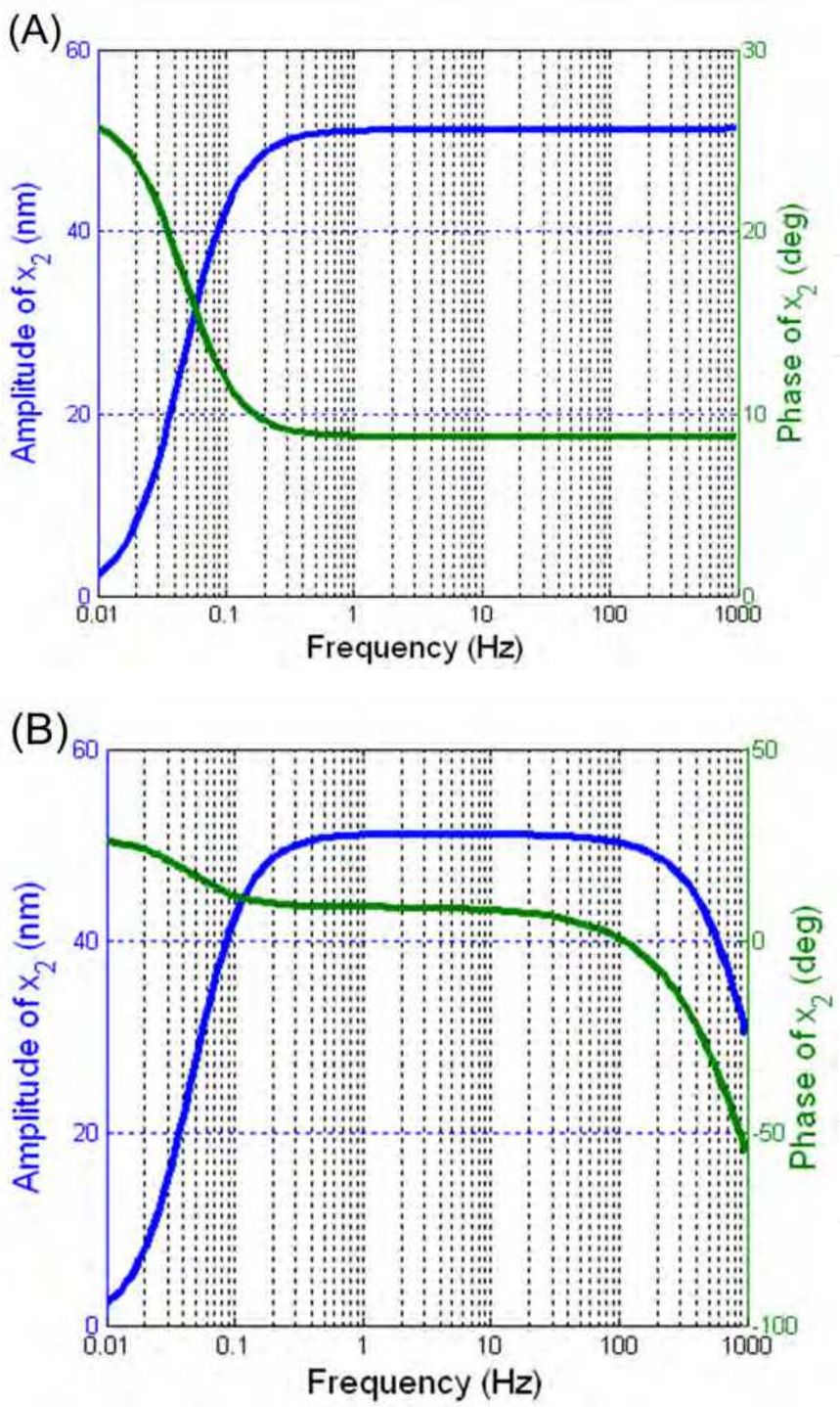

Fig. 9. The dynamic response of mass 2 for the case (A) no air damping and for (B) significant air damping

As can be seen the maximum displacement is only 52 nm. This is despite the relatively large voltage that was applied to the actuating comb-drive. The advantage of this is that it is very

likely that any non-linear effects are negligibly small and that the strains in the liquid are sufficiently low that linear viscoelastic theory is valid (Bird et al., 1987). The issue is that it may be too small to be measured. Ignoring parasitic capacitances, the change in the capacitance of the sensing comb-drive is:

$$dC(t) = n\frac{\varepsilon t}{g}x_2(t) \tag{75}$$

In this instance, the capacitance is nominally c.a. 39.8 pF. The sensitivity of the comb-drive, given by eq. 76, can be shown to be 0.44 pF/μm, which is low given that displacements are in the nanometre regime.

$$\frac{\partial C}{\partial x} \approx n\frac{\varepsilon t}{g} \tag{76}$$

This is one of the main problems with this sort of device: you need to apply large voltages to achieve reasonable displacements and it still results in small changes in capacitances which may be difficult to measure, as can be seen in Fig. 10. Fortunately, new capacitance measurement chips with accuracies as good as 4 aF/√Hz (Irvine Sensors, n.d.) are commercially available, making these devices viable.

Another issue is the effect of air damping. Unless the comb-drives are sealed in a vacuum, it is likely that air-damping will be significant and will have to be included in the analysis using eqs. 11 and 12 rather than 13 and 14 (see Fig. 9). Unfortunately, in cases of complicated geometries such as this, damping is difficult to calculate. Even numerical analysis using CFD or FEA is unlikely to be accurate due to the number of assumptions and simplifications needed to get convergence (Ye et al., 2003). However, due to the comprehensive modelling, it is quite a simple task to curve fit to experimental data like that shown in Fig. 9, given a model fluid in the channel whose rheometry is well known, and ascertain the mechanical parameters more accurately. In practice it may be necessary to calibrate the rheometer in this manner anyway due to the variability of MEMS fabrication technologies in order to establish real values for the masses and stiffnesses.

The purpose of this chapter was to describe the complete system analysis of a new kind of coupled-mass microrheometer and show how such a device can be integrated into a real production process. The main issue is that in the installation of a sensor into a commercial process there should be no disruption or chance of contamination of the main process flow line. Naturally, issues such as space constraints and cleaning cycles need to be addressed as well. A possible lay-out is shown in Fig. 11. Here the microrheometer is connected externally to the main process flow line and to cleaning lines via electrically actuated three-way valves. Both the fluid to be tested and cleaning fluid are likely to need to be pumped into the microfluidic channel as the pressure required to push the fluid through the device will possibly be higher than that available in the main lines due to the constrictions in the channel. It can be imagined that at certain intervals of time, process fluid will be pumped into the channel, a frequency sweep performed and the channel washed clean while the data is analysed. Overall, as the device is channel-based rather than based on a liquid bridge, integration into automated commercial process lines is simple and allows for real-time, high-throughput analysis that can be used for quality control and product optimisation.

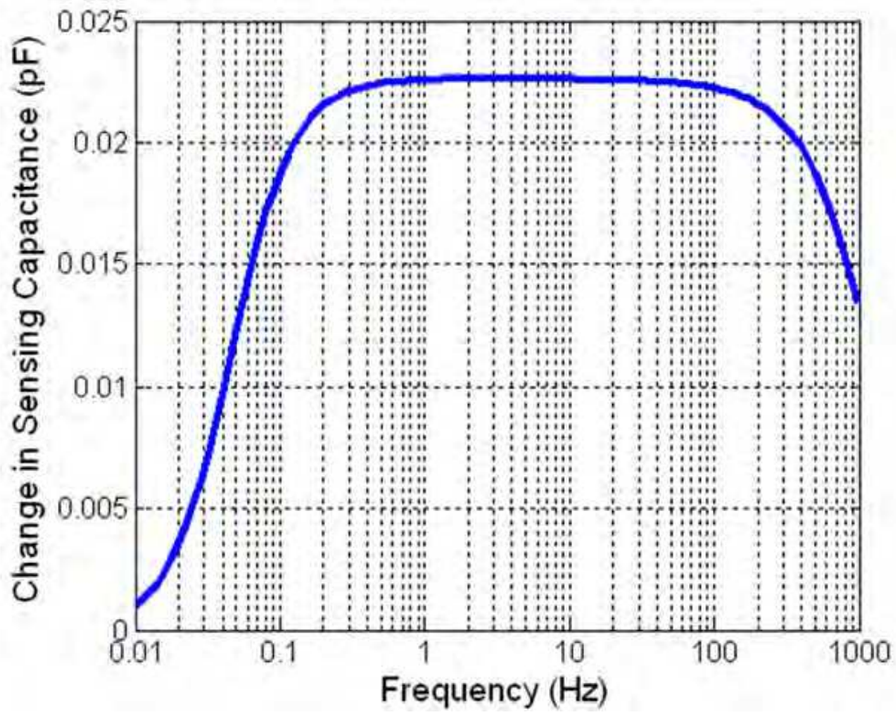

Fig. 10. Resultant change in amplitude of capacitance of sensing comb-drive

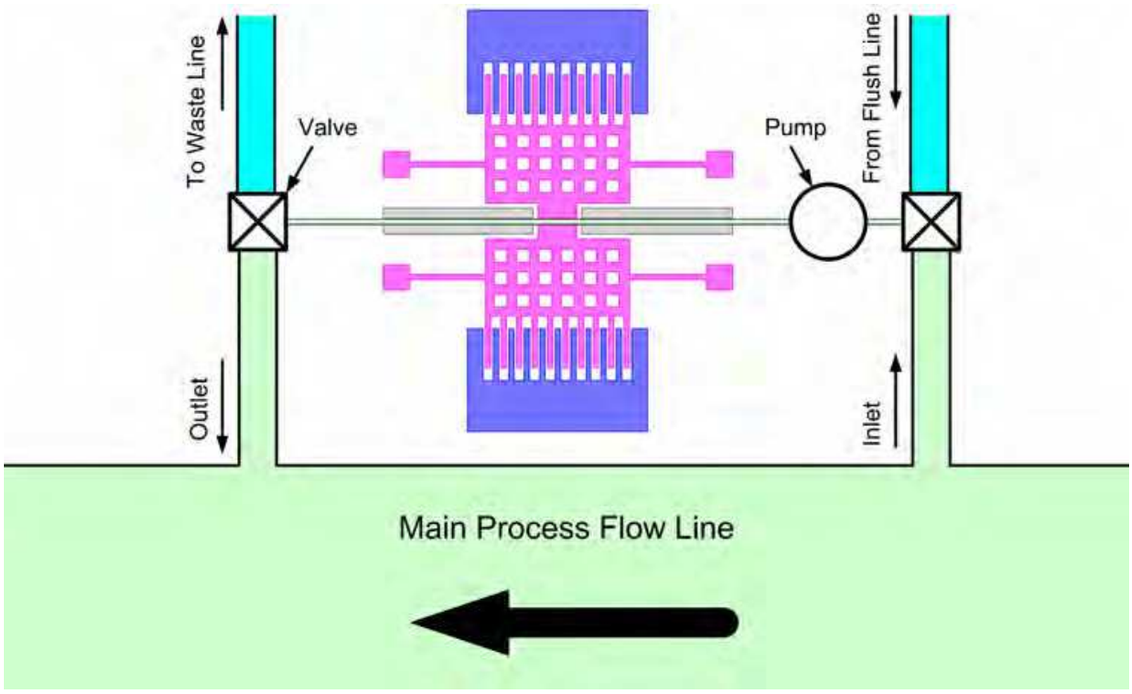

Fig. 11. Potential layout for integration of sensor into a commercial process flow line

5. Conclusion

A deterministic method of measuring viscoelastic fluid properties using a new kind of coupled-mass microrheometer has been shown. The fluid mechanics has been fully analysed as a viscoelastic squeeze flow problem and coupled with dynamical and electrical analysis. It has also been shown how such a device can be integrated into a real production process.

6. Acknowledgments

The author would like to thank Bethany Hanson for proofreading this chapter.

7. References

Bell, D., Binding, D. M. & Walters, K. (2005). The Oscillatory Squeeze Flow Rheometer - Comprehensive Theory and a New Experimental Facility, *Rheologica Acta*, Vol.46, No.1, (May 2006), pp. 111-121, ISSN 0035-4511

Bird, R. B., Armstrong, R. C. & Hassager, O. (1987). *Dynamics of Polymeric Liquids, Fluid Mechanics Vol. 1,* 2nd Ed., Wiley-Interscience, ISBN 047180245X, New York

Cheneler, D., Bowen, J., Ward, M. C. L. & Adams, M. J. (2011). Principles of a Micro Squeeze Flow Rheometer for the Analysis of Extremely Small Volumes of Liquid, *Journal of Micromechanics and Microengineering,* Vol.21, No.4, (April 2011), 045030, ISSN 0960-1317

Christopher, G. F., Yoo, J. M., Dagalakis, N., Hudson, S. D. & Migler, K. B. (2010). Development of a MEMS based Dynamic Rheometer, *Lab on a Chip*, Vol.20, (August 2010), pp. 2749-2757, ISSN 1473-0197

Crecea, V., Oldenburg, A. L., Liang, X., Ralston, T. S. & Boppart, S. A. (2009). Magnetomotive Nanoparticle Transducers for Optical Rheology of Viscoelastic Materials, *Optical Express*, Vol.17, No.25, (December 2009) pp. 23114-23122, ISSN 1094-4087

Denn M. M. & Marrucci, G. (1999). Squeeze Flow between Finite Plates, *Journal of Non-Newtonian Fluid Mechanics*. Vol. 87, pp. 175–178, ISSN 0377-0257

Engmann, J., Servais, C. & Burbidge, A. S. (2005). Squeeze Flow Theory and Applications to Rheometry: A Review, *Journal of Non-Newtonian Fluid Mechanics*, Vol. 132, No. 1-3, (December 2005), pp. 1-27, ISSN 0377-0257

Hansen, C. & Quake, S. R. (2003). Microfluidics in Structural Biology: Smaller Faster . . . Better. *Current Opinion in Structural Biology,* Vol.13, (October 2003), pp. 538–454, ISSN 0959-440X

Irvine Sensors (n.d.). MS3110 Universal Capacitive Readout™ IC, 23.08.2011, Available from http://www.irvine-sensors.com/pdf/MS3110%20Datasheet%20USE.pdf

Kumble, K. D. (2003). Protein Microarrays: New Tools for Pharmaceutical Development, *Analytical and bioanalytical chemistry*, Vol.377, (July 2003), pp. 812–819, ISSN 1618-2642

Lee, K. B. (2011). *Principles of Microelectromechanical Systems*, Wiley-IEEE, ISBN 0470466340, Singapore

Macosko, C. W. (1994). *Rheology: Principles, Measurements, and Applications*, Wiley-VCH, ISBN 0471185752, New York

Rao, S. S. (2010). *Mechanical Vibrations*, Prentice Hall, ISBN 0132128195, New York

Reynolds, O. (1886). On the Theory of Lubrication and Its Application to Mr. Beauchamp Tower's Experiments, Including an Experimental Determination of the Viscosity of Olive Oil, *Philosophical Transactions of the Royal Society of London*, Vol. 177, (February 1886), pp. 157-234, ISSN: 02610523

Strauss, W. A. (2007). *Partial Differential Equations*, Wiley, ISBN 0470054565, New York

Sujatha, K. S., Matallah, H., Babaai, M. J. & Webster, M. F. (2008). Modelling Step-Strain Filament-stretching CaBER-type using ALE Techniques, *Journal of Non-Newtonian Fluid Mechanics.*, Vol.148, (January 2008), pp. 109-121, ISSN 0377-0257

Walters, K. (1975). *Rheometry*, Chapman & Hall, ISBN 0412120909, London

Wei, X., Anthony, C., Lowe, D. & Ward, M. C. L. (2009). Design and Fabrication of a Nonlinear Micro Impact Oscillator, *Procedia Chemistry*, Vol.1, (September 2009), pp. 855–858, ISSN 1876-6196

Ye, W., Wang, X., Hemmert, W., Freeman, D. & White, J. (2003). Air Damping in Laterally Oscillating Microresonators: A Numerical and Experimental Study, *Journal of* Microelectromechanical Systems, Vol. 12, No. 5, (October 2003), pp. 557-566, ISSN 1057-7157

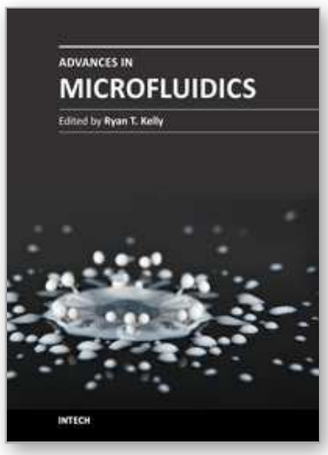

Advances in Microfluidics

Edited by Dr. Ryan Kelly

ISBN 978-953-51-0106-2
Hard cover, 250 pages
Publisher InTech
Published online 07, March, 2012
Published in print edition March, 2012

Advances in Microfluidics provides a current snapshot of the field of microfluidics as it relates to a variety of sub-disciplines. The chapters have been divided into three sections: Fluid Dynamics, Technology, and Applications, although a number of the chapters contain aspects that make them applicable to more than one section. It is hoped that this book will serve as a useful resource for recent entrants to the field as well as for established practitioners.

How to reference

In order to correctly reference this scholarly work, feel free to copy and paste the following:

David Cheneler (2012). Analysis of a Coupled-Mass Microrheometer, Advances in Microfluidics, Dr. Ryan Kelly (Ed.), ISBN: 978-953-51-0106-2, InTech, Available from: http://www.intechopen.com/books/advances-in-microfluidics/analysis-of-a-coupled-mass-microrheometer

INTECH
open science | open minds

InTech Europe
University Campus STeP Ri
Slavka Krautzeka 83/A
51000 Rijeka, Croatia
Phone: +385 (51) 770 447
Fax: +385 (51) 686 166
www.intechopen.com

InTech China
Unit 405, Office Block, Hotel Equatorial Shanghai
No.65, Yan An Road (West), Shanghai, 200040, China
中国上海市延安西路65号上海国际贵都大饭店办公楼405单元
Phone: +86-21-62489820
Fax: +86-21-62489821

IntechOpen